Detecting concealed information using functional near-infrared spectroscopy (fNIRS) combined with skin conductance, heart rate, and behavioral measures

Di Wang | **Chongxiang Wang** | **Xingyu Yi** | **Liyang Sai** | **Genyue Fu** | **Xiaohong Allison Lin**

Department of Psychology, Hangzhou Normal University, Hangzhou, China

Correspondence
Xiaohong Allison Lin, Department of Psychology, Hangzhou Normal University, Hangzhou, China.
Email: xiaohonglin@hznu.edu.cn, zhulin24show@hotmail.com

Abstract

In this study, brain imaging data from functional near-infrared spectroscopy (fNIRS) associated with skin conductance response (SCR), heart rate (HR), and reaction time (RT) were combined to determine if the combination of these indicators could improve the efficiency of deception detection in concealed information test (CIT). During the CIT, participants were presented with a series of names and cities that served as target, probe, or irrelevant stimuli. In the guilty group, the probe stimuli were the participants' own names and hometown cities, and they were asked to deny this information. Our results revealed that probe items were associated with longer RT, larger SCR, slower HR, and higher oxy-hemoglobin (HbO) concentration changes in the inferior prefrontal gyrus (IFG), middle frontal gyrus (MFG), and the superior frontal gyrus (SFG) compared with irrelevant items for participants in the guilty group but not in the innocent group. Furthermore, our results suggested that the combination of RT, SCR, HR, and fNIRS indicators could improve the deception detection efficiency to a very high area under the ROC curve (0.94) compared with any of the single indicators (0.74–0.89). The improved deception detection efficiency might be attributed to the reduction of random error and the diversiform underlying the psychophysiological mechanisms reflected by each indicator. These findings demonstrate a feasible way to improve the deception detection efficiency by using combined multiple indicators.

KEYWORDS
concealed information test, deception detection, fNIRS, heart rate, reaction time, SCR

1 | INTRODUCTION

Deception is widespread in our daily life and people may deceive for various reasons, such as evading punishment and gaining self-benefits, as well as prosocial motivation (DePaulo et al., 1996). However, most deception have negative effects and could further pose a threat to the safety and stability of society (Ganis et al., 2011). To date, studies on deception detection have attracted significant attention in various fields, and feasible future applications

Di Wang and Chongxiang Wang are the authors contributed equally to this study.

require more reliable and effective methods for detecting deception (Ben-Shakhar et al., 2002; Gronau et al., 2005; Matsuda et al., 2012; Nahari & Ben-Shakhar, 2011; Zhang et al., 2017). Deception detection has traditionally relied on the use of single measurement, including behavioral, psychophysiological, or neuroimaging measures, as indicators, with some of these approaches achieving detection efficiencies higher than 80% (Meijer et al., 2016). Although some studies have already applied the use of multiple measurements in different deception detection paradigms, the efficiencies of these strategies have rarely been addressed with combining fMRI (fNIRS) based brain imaging data and physiological measures (Bhutta et al., 2015; Gamer et al., 2007). The present study aimed to investigate whether combining brain activity from fNIRS, skin conductance, heart rate, and behavioral measures could enhance deception detection efficiency in a three-stimulus concealed information test.

The concealed information test (CIT; Lykken, 1960) has been used in both laboratory research and the judicial field for distinguishing between guilty and innocent participants (Meijer et al., 2007). Generally, three stimuli are included in the standard CIT: (1) Crime-related items (also called probe items) that include information related to criminal behavior which is usually hidden by criminals. (2) Irrelevant items that are unrelated to criminal behavior and with which both criminals and innocents are unfamiliar. (3) Target items that are additional irrelevant messages requiring different reactions from the irrelevant and probe items. These items are used to maintain the attention of the participants (Rosenfeld et al., 2006).

The reaction time (RT) based CIT has been shown to successfully distinguish between participants with and without criminal knowledge (Ben-Shakhar, 2012; Farwell & Donchin, 1991; Rosenfeld et al., 2004, 2006). The results of meta-analysis studies about lie detection techniques indicated that the mean effect size (Cohen's d) is 1.26 for RT, which already higher than Respiration Line Length (Cohen's $d = 1.11$) and Heart Rate (Cohen's $d = 0.89$) (Meijer et al., 2014; Suchotzki et al., 2017). The rationale for RT-based CIT can be explained from the cognitive perspective which holds that deception is more cognitively demanding than telling the truth (Verschuere et al., 2011; Vrij, 2008).

Physiological indicators based on the autonomic nervous system have been historically used in the CIT paradigm to detect concealed information (Iacono & Lykken, 1997). Specifically, different psychological processes lead to physiological changes that can be measured (Synnott et al., 2015). Skin conductance responses (SCRs), respiration line length (RLL), and heart rate (HR) are the most common indicators examined with a polygraph (Gamer et al., 2008). In the physiological-measure-based CIT, a typical response pattern for a person who recognizes crime-related information includes larger SCRs, a shorter RLL, and a decelerated HR, which is also called the CIT effect. Studies have recently suggested that these physiological responses are driven by different mechanisms and could be explained by the response fractionation model (Klein Selle et al., 2019). The increased SCR reflects an orienting response, whereas RLL and HR reflect attempts to inhibit arousal (AI; Klein Selle et al., 2016; Verschuere et al., 2007).

The development of brain imaging technologies such as functional magnetic resonance imaging (fMRI) has made it possible to better understand the neurological basis of deception by measuring the activity of the central nervous system (Bles & Haynes, 2008; Gamer et al., 2007; Sai et al., 2021). Most previous researches have adopted the differentiation of deception paradigm (DDP), which focused on a comparison between deception and truth (Gamer et al., 2012). However, only a few of studies have used fMRI-based CIT to explore the neural correlates of the CIT and whether brain activities elicited during the CIT can be used to distinguish guilty participants from innocent participants (Gamer et al., 2007, 2012; Suchotzki et al., 2015). The mechanism of fMRI-based CIT has been explained as response inhibition (Suchotzki et al., 2015), although the role of the orienting response has also been discussed (Gamer et al., 2012). Furthermore, fMRI has several limitations, such as high costs, noisy acquisition, and restrictions on subjects which reduce the ecological validity of this approach for forensic applications (Farah et al., 2014).

Functional near-infrared spectroscopy (fNIRS) has shown significant potential in neuroimaging as it is portable, cost-effective, quiet, with a high tolerance rate and a high temporal resolution compared with fMRI (Lin et al., 2017, 2018; Liu et al., 2017). Given these advantages, a number of studies have used fNIRS to examine the neural correlates of deception in relatively natural and realistic settings, and these studies consistently found that deception is associated with greater activity in the prefrontal cortex (PFC), specifically, in the SFG, MFG, and IFG (Ding et al., 2013, 2014; Lin et al., 2021; Sai et al., 2014; Tian et al., 2009). However, only a small number of studies have used fNIRS to detect deception (Bhutta et al., 2015; Sai et al., 2014).

Multiple autonomic measurements have been combined to detect concealed information, and most studies showed improved detection efficiencies with combinations of autonomic responses compared with single measurement (see a review, Gamer, 2011). With the development of event-related brain potential (ERP) based CIT, ERP has been combined with autonomic-based CIT (Gamer & Berti, 2010; Matsuda et al., 2009), with

the combination of ERP and autonomic measurements achieving better discrimination accuracy (Gamer & Berti, 2010; Matsuda et al., 2011). This indicates that combining measurements from the autonomic central nervous systems result in improved detection validity. In addition, fMRI also has been used in CIT associated with autonomic indictors (Gamer et al., 2007, 2012; Suchotzki et al., 2015). However, most of these fMRI-based studies (e.g., Suchotzki et al., 2015) did not involve the calculation of the combined detection efficiency, while others found that the addition of autonomic measures to fMRI had little effect on the diagnostic ability (Kozel et al., 2009). Another brain activation-based instrument, fNIRS, also has been combined with autonomic measures to detect concealed information, and Bhutta et al. (2015) demonstrated the feasibility of combining fNIRS and the physiological measurement for detecting deception, showing a detection efficiency of 86.5%, which was higher than that of single measure. Sai et al. (2014) used the CIT paradigm and required guilty participants to conceal crime-related information from a mock crime. The fNIRS detection efficiency of guilty participants versus innocent participants was 75%, and when fNIRS was combined with RT, the efficiency reached 83.3%. As previous studies have suggested (Gamer, 2011), behavioral measurement, autonomic measurements, and brain activation-based measures are likely to be associated with different psychophysiological mechanisms. The combination of measures thus reduces random error and enhances reliability, suggesting that the combination of multiple measures may elevate the detection efficiency of the CIT.In the current study, we combined behavioral data (RT), physiological data (skin conductance response, SCR; heart rate, HR), and brain imaging data (fNIRS data) to detect concealed information in a standard three-stimulus CIT. Specifically, RT reflects cognitive effort, SCR reflects the orienting response, HR reflects arousal inhibition, and fNIRS reflects response inhibition. This allows the integration of autonomic and central nervous system data for deception detection. The combination of multiple measures also could reduce the random error and enhance the reliability. To the best of our knowledge, this is the first study using fNIRS imaging data combined with RT, SCR, and HR to detect concealed information. We hypothesized that, RT, HR, SCR, and imaging data from fNIRS recordings could distinguish probe and irrelevant items in the guilty group but not the innocent group. We also expected that RT, HR, SCR, and fNIRS could distinguish guilty from innocent participants, significantly above the level of chance. Also, given that the association of multiple indicators with variable mechanisms and that the combination of multiple measures

could reduce random error, we expected the combination of RT, SCR, and HR with fNIRS measurements could improve the deception detection classification of a single indicator resulting in a better classification method.

2 | METHOD

2.1 | Participants

Seventy-two right-handed students (34 male) from the Hangzhou Normal University participated in this study, with an age range of 17–27 ($M = 21.2$, $SD = 1.9$ years). All participants had a normal or corrected-to-normal vision and were without any history of psychiatric or neurological disorders. Participants read and signed an informed consent before the experiment and could quit the task at any time without penalty. The study was conducted under guidelines approved by the ethics committee of Hangzhou Normal University.

The data from one participant were excluded from analysis due to the participant's misunderstanding of the instructions and pressing the inverse buttons when presented with her name and hometown. Data from four participants were excluded because of technical problems with having no available triggers. Data from five participants were excluded due to the non-responsivity of the SCR data, while data from two participants were excluded because of low signal quality of the fNIRS data. Finally, 60 available participants' data were used for the analysis (30 male).

2.2 | Procedure

Before the task, the participants first signed an informed consent form and were then presented with a list of names and cities. Participants were instructed to select those with special personal meaning (e.g., the names of parents or friends, cities where their schools were located). These two examples of unselected information (two categories: name or city) were randomly used as irrelevant items in the CIT task (Verschuere et al., 2010). The participants were then randomly divided into innocent or guilty groups in the task. A three-stimulus CIT design was used in this study, containing target, probe, and irrelevant stimuli. For all participants, a Chinese star's name ("Dehua Liu") and his hometown ("Hong Kong") were used as targets. Four other names and four cities were assigned as irrelevant items. For the guilty group, the participant's own name and hometown were the probe stimuli, whereas for the innocent group, the probe stimuli were an irrelevant name

and city. Participants were unfamiliar with all the irrelevant names and cities.

Before the CIT test, a cover story was told to all participants, that an information leakage incident occurred in an intelligence agency, and the name and hometown information of the spy were leaked. Then, the participants were asked to imagine a scene in which they were suspected to be spies when preparing to board a plane at an airport and were required to prove their innocence through a lie detector. During the CIT test, the participants were presented with a sequence of names and cities and were asked to press the left button as soon as possible when they recognized the stimuli and to press the right button when they did not recognize the stimuli (the meaning of buttons had been counterbalanced). For example, when they saw the target stimuli Dehua Liu and Hong Kong, they should press the left button to indicate that they recognized these stimuli. When the participants in the guilty group were presented with probe stimuli, they were asked to press the right button to deny the recognition of these stimuli and avoid being detected as spies. The participants were thus lying as they recognized the stimuli. All stimuli were presented in a pseudo-random order without the repetition of two consecutive items.

During the CIT test, participants were seated comfortably in front of a computer to avoid physical movements and to ensure the accuracy of the results. There were two targets, two probes, and eight irrelevant items in the test. Each item was repeated eight times, thus the whole task contained 96 trials. At the beginning of each trial, a fixation was presented for 1 s and the stimulus item was presented for 1 s with an inter-stimulus interval (ISI) of 14 s (Figure 1a). If the participants did not respond within 1 s, feedback ("TOO SLOW") was presented for 4 s. The experiment ended automatically if the participants had missed five responses in the task. The whole experiment lasted for approximately 26 min.

2.3 | Data acquisition for concurrent fNIRS and physiological recordings

The experiment was performed using a Continuous Wave (CW6) fNIRS system (Techen, Inc., Milford, MA, USA) with six laser sources and fourteen optical detectors. In the present study, a homemade plastic patch was used to acquire fNIRS data with probes positioned according to the international 10–20 system so that the lowest probes were aligned with the Fp1-Fp2 line. The optodes were symmetrically arranged in a $7 \times 30 \text{cm}^2$ area with a 3-cm distance between each source and detector. The diffuse NIR light from each source through the cortical region was acquired by its nearest detector and 24 source-detector pairs (channels) were measured in total (Tian et al., 2009; Figure 1b). The sampling rate for the acquisition of the fNIRS data was 25 Hz. Moreover, the 3D-magnetic space digitizer Patriot Digitizer (Polhemus Inc., Colchester, Vermont, USA) was used for a standard participant (head size: 59 cm) to obtain the 3D spatial information of each optode. NIRS-SPM software was used to estimate the
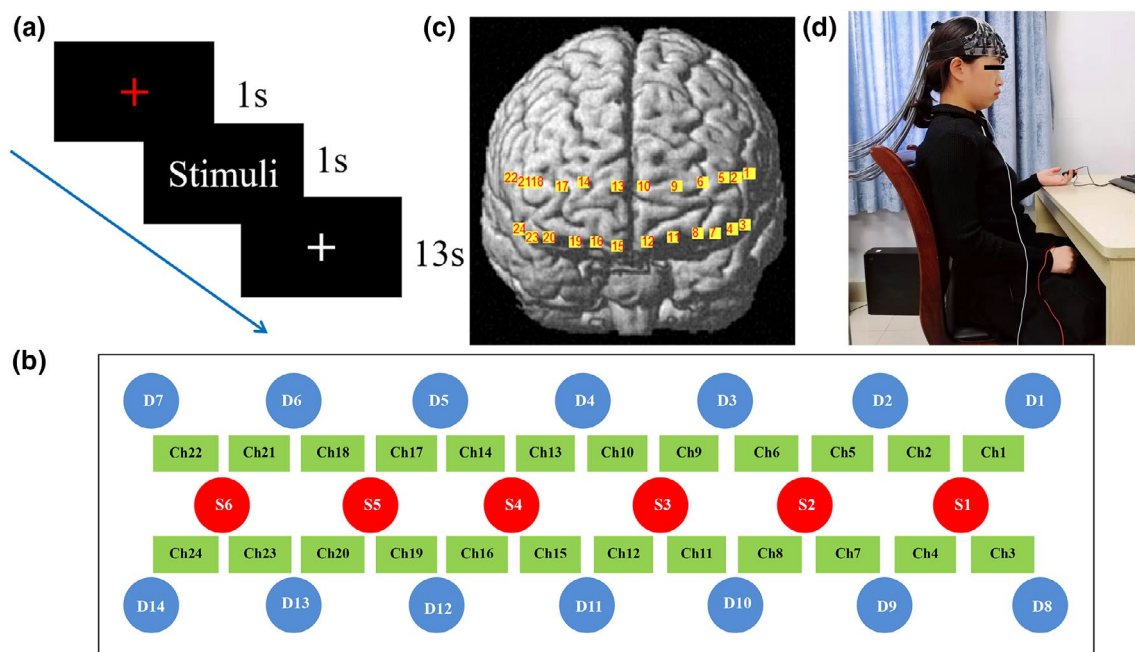

FIGURE 1 (a) Schematic illustration of a single trial for the concealed information test task. (b) The arrangements of the optodes for the fNIRS system (the red circles represent sources, the blue circles represent detectors, and the green rectangles represent the fNIRS channels). (c) The estimated locations of the 24 fNIRS channels on the prefrontal cortex. (d) The experimental setup

3D location in the Montreal Neurological Institute (MNI) space (Singh et al., 2005), and the 3D spatial coordinates of 24 channels are shown in Figure 1c.

The electrodermal and electrocardiogram (ECG) data of the participants were acquired using a BIOPAC MP160 system (BIOPAC Systems, Inc., Goleta, CA, United States). SCR measures were obtained using two Ag/AgCl electrodes (TSD203) filled with GEL101 that were placed on the phalanges of the index and middle fingers of the left hand. All the participants washed their hands prior to the attachment of the electrodes. ECG measurements were acquired using three electrodes placed in a lead II configuration. The negative electrode was placed below the right clavicle, the positive electrode was placed on the left lower abdomen, and the ground electrode was placed on the right lower abdomen. The BIOPAC MP160 system was set at 1 Hz low-pass band for SCR signals and at 1–35 Hz for ECG signals, and the SCR, ECG signals were sampled at 1000 Hz using the AcqKnowledge v. 4.1 (BIOPAC Systems, Inc. Goleta, CA, USA) software and the signals were displayed on a laptop. E-prime 2.0 software was used for stimulus presentation during the experiment.

2.4 | Data analysis

2.4.1 | fNIRS data analysis

Homer2 software (Huppert et al., 2009) was used for fNIRS data preprocessing. The raw data were first converted to optical density changes and then converted to oxyhemoglobin (HbO) and deoxyhemoglobin (HbR) concentration changes using the modified Beer–Lambert Law (Cope & Delpy, 1988). The HbO and HbR changes were then filtered with a low-pass filter of 0.2 Hz and a high-pass filter of 0.01 Hz. In this study, only HbO changes were analyzed as the change in HbO is the more sensitive indicator of regional cerebral blood flow changes (Homae et al., 2007). The duration of each trial was 15 s, containing a 1-s prior onset period, a 1-s stimulus period, and a 13-s recovery period. We calculated the run-averaged HbO concentrations and the grand-averaged HbO data for the probe and irrelevant stimuli of guilty/innocent groups. The mean values of 5–9, 4–10, and 1–14 s of the run-averaged HbO data for each participant were extracted by each channel for statistical analyses as the HbO peaks were located within these time windows. As the results from these three time windows were almost same, we chose 5–9 s window as the representative time window for fNIRS HbO changes for further analyses. All p-values of the F-test were corrected using a false-discovery-rate (FDR, $p < .05$; Singh & Dan, 2006). Statistical analyses for fNIRS data were conducted using SPSS 20.0. Also, the HbO changes were mapped using the BrainNet Viewer (Xia et al., 2013) tool to show the brain imaging activity of the probe/irrelevant items in the guilty/innocent groups.

2.4.2 | Physiological responses

For the SCR data, AcqKnowledge v.4.1 (BIOPAC Systems, Inc., Goleta, CA, United States) was used to calculate the peak-to-peak amplitude, defined as the maximal change between the peaks (Yu et al., 2019). For each participant, the mean values of the peak-to-peak amplitude during 1–5 s were calculated.

For ECG data, AcqKnowledge v.4.1 and MATLAB (The MathWorks, Natick, MA, USA) were used to detect the R waves and R peaks and to calculate the distance between them with an artifact detection and rejection procedure (De Clercq et al., 2006; Klein Selle et al., 2016). Prior to analysis, the inter-beat intervals were converted to HR in beats per minute (bpm) per real-time epoch (1-s). These second-by-second post-stimulus HR values were baseline-corrected by subtracting the average HR value in the 3-s preceding stimulus onset, resulting in 10 post-stimulus difference scores ($\triangle$HR). It has been demonstrated that the average values of all $\triangle$HR scores were better than the minimum of all $\triangle$HR scores as a detection measure (Gamer et al., 2008; Klein Selle et al., 2016).

Because of individual differences in physiological responsivity, within-subject standard Z-scores were calculated separately for SCR and HR (the target item was excluded from the standardization, Klein Selle et al., 2019). For SCR and HR measures, those responses were removed if the Z-scores were larger than 5 or smaller than −5. Furthermore, participants whose response fell below 0.01 of the standard deviation of the raw SCR scores were considered to be non-responders and their data were eliminated from all SCR analyses (Geven et al., 2018). Finally, a total of 1.1% of HR and 1.3% of SCR responses to the stimuli were eliminated due to excessive movements and outliers.

For SCR and HR data, the probe item data were used as dependent variables in the following analyses in order to investigate whether the SCR and HR indicators could distinguish the guilty group from innocent participants (Klein Selle et al., 2016).

3 | RESULTS

3.1 | Behavioral results

A 2×2 ANOVA on the accuracy of the participant responses was performed using the group (guilty vs.

innocent) as a between-subject factor and the item type (probe, irrelevant item) as a within-subject factor to reveal the significance of the stimulus type, $F(1, 58) = 8.14$, $p < .05$, $\eta^2 = 0.12$), and interactions between the stimulus type and the group, $F(1, 58) = 14.19$, $p < .001$, $\eta^2 = 0.20$). The group was found to have no significant effect, $F(1, 58) = 1.02$, $p > .05$.

The RT results revealed a significant effect of the item type, $F(1, 58) = 26.57$, $p < .001$, $\eta^2 = 0.31$, as well as a significant interaction between the item type and the group, $F(1, 58) = 21.90$, $p < .001$, $\eta^2 = 0.27$ (Figure 2a). A simple effect test showed that the RTs to the probe items in the guilty group were significantly longer than those to the irrelevant items, $F(1, 58) = 48.36$, $p < .001$, $\eta^2 = 0.46$. However, the RTs to both probe and irrelevant items in the innocent group did not reach statistical significance, $F(1, 58) = 0.11$, $p > .05$.

3.2 | fNIRS results

A 2×2 mixed measure ANOVA was performed with a within-subject variable (stimulus type: probe vs. irrelevant) and a between-subject variable (group: guilty vs. innocent). The results are summarized in Tables 1 and S1. Significant effects of stimulus type were observed in channels 2, 3, 4, 5, 6, 7, 8, 9, 10, 11, 12, 13, 14, 15, 16, 17, 18, 19, 20, 21, 23, and 24 ($Fs \geq 4.44$, $ps \leq .04$, $\eta^2 s \geq 0.07$, FDR corrected). The group had no significant effect in the 24 channels after FDR correction. Statistical analysis of the data revealed significant interactions between the stimulus type and group in channels 1, 2, 4, 5, 6, 7, 8, 9, 10, 11, 12, 13, 14, 15, 16, 17, 18, 19, 20, 21, 22, 23, and 24 ($Fs \geq 4.83$, $ps \leq .03$, $\eta^2 s \geq 0.08$, FDR corrected, Table 1). The data showed that the participants in the guilty group exhibited significantly higher HbO changes in response to probe stimuli compared to irrelevant stimuli in channels 1, 2, 4, 5, 6, 7, 8, 9, 10, 11, 12, 13, 14, 15, 16, 17, 18, 19, 20, 21, 22, 23, and 24 ($Fs \geq 10.95$, $ps \leq .01$, $\eta^2 s \geq 0.16$). However, no significant differences in the HbO changes between the probe and irrelevant stimuli were observed for the innocent group. The averaged HbO changes of each channel for the probe and irrelevant stimuli from the guilty and innocent groups are shown in Figure 3. To image the brain activation for probe and irrelevant stimuli conditions in the guilty and innocent groups, the HbO images were generated and displayed on a brain template, as shown in Figure 4.

3.3 | Physiological results

Independent t-tests were conducted for each physiological indicator (SCR and HR) with a between-subject variable (group: guilty vs. innocent), and dependent variable (z-scores of the probe items).

For the SCR data, the results of independent t-tests showed that there was a significant difference between the SCR in response to probe items between the guilty and innocent groups, $t(59) = 6.19$, $p < .001$, Cohen's $d = 1.60$, indicating that the SCR to the probe item in the guilty was significantly larger than that in innocent group (Figure 2b).

For the HR data, the results of independent t-tests showed that there was a significant difference between the HR in response to probe items between the guilty and innocent groups, $t(59) = -3.56$, $p < .01$, Cohen's $d = -0.92$, indicating that the HR response to the probe in the guilty group was significantly shorter than that in the innocent group (Figure 2c).
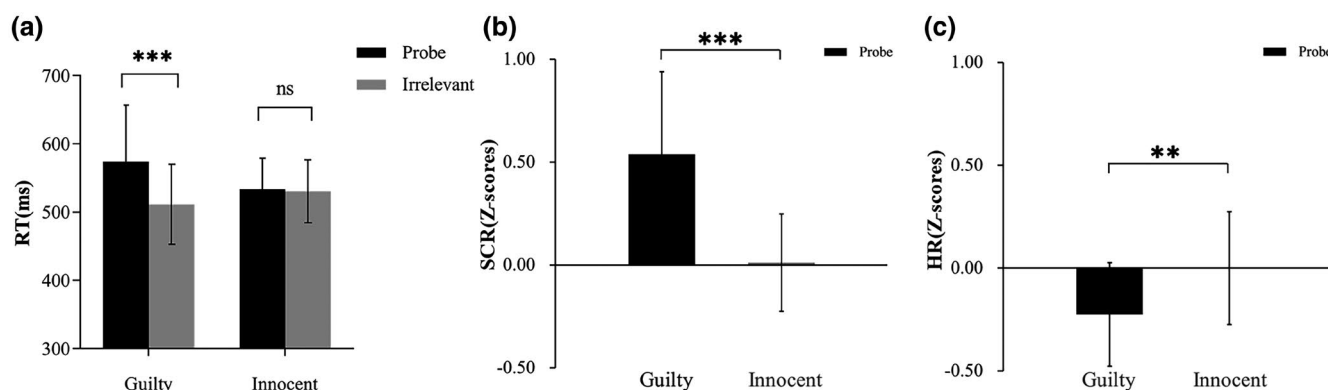
FIGURE 2 (a) The reaction time (RT) to the probe and irrelevant items in the guilty and innocent groups. (b) The Z-scores of the skin conductance response (SCR) to the probe items of the guilty and innocent participants. (c) The Z-scores of heart rate (HR) to the probe items of the guilty and innocent participants. Note: $^*p < .05$, $^{**}p < .01$, $^{***}p < .001$

TABLE 1 Statistical analysis using fNIRS oxyhemoglobin (HbO) changes

Channels	MNI coordinates			Brain regions	Probability	Group × stimulus	AUC
	X	Y	Z				
Ch 1	−53	38	13	Left IFG (BA45)	0.92	$F = 7.49^{*}$	0.70^{**}
Ch 2	−48	48	12	Left IFG (BA46)	0.54	$F = 18.29^{***}$	0.80^{***}
Ch 3	−52	42	−9	Left IFG (BA46)	0.87	$F = 3.85$	N/A
Ch 4	−46	51	13	Left IFG (BA47)	0.69	$F = 21.56^{***}$	0.80^{***}
Ch 5	−41	57	11	Left MFG (BA46)	0.98	$F = 23.80^{***}$	0.85^{***}
Ch 6	−32	65	9	Left SFG (BA10)	0.52	$F = 15.96^{***}$	0.79^{***}
Ch 7	−39	58	14	Left MFG(BA47)	0.7	$F = 22.75^{***}$	0.85^{***}
Ch 8	−30	62	−15	Left MFG (BA11)	0.9	$F = 21.31^{***}$	0.85^{***}
Ch 9	−20	72	9	Left SFG (BA10)	0.99	$F = 13.58^{***}$	0.77^{***}
Ch 10	−3	70	8	Left SFG (BA10)	0.76	$F = 14.36^{***}$	0.79^{***}
Ch 11	−18	66	−17	Left MFG (BA11)	0.57	$F = 13.70^{***}$	0.78^{***}
Ch 12	−6	68	−18	Left SFG (BA11)	0.36	$F = 10.92^{***}$	0.73^{**}
Ch 13	9	74	8	Right SFG (BA10)	0.93	$F = 8.34^{**}$	0.73^{**}
Ch 14	25	71	9	Right SFG (BA10)	0.99	$F = 13.09^{**}$	0.76^{**}
Ch 15	8	68	−20	Right SFG (BA11)	0.56	$F = 9.84^{**}$	0.73^{**}
Ch 16	18	66	−18	Right MFG (BA11)	0.52	$F = 10.82^{**}$	0.72^{**}
Ch 17	34	66	8	Right SFG (BA10)	0.64	$F = 12.93^{**}$	0.78^{***}
Ch 18	46	56	9	Right MFG (BA46)	0.99	$F = 16.21^{***}$	0.80^{***}
Ch 19	28	62	−18	Right MFG (BA11)	0.97	$F = 13.07^{**}$	0.77^{***}
Ch 20	40	57	−17	Right MFG (BA47)	0.97	$F = 16.54^{***}$	0.79^{***}
Ch 21	53	44	10	Right IFG (BA45)	0.54	$F = 9.73^{**}$	0.81^{***}
Ch 22	59	33	12	Right IFG (BA45)	1	$F = 4.83^{*}$	0.69^{*}
Ch 23	49	49	−16	Right IFG (BA47)	0.6	$F = 11.38^{**}$	0.74^{**}
Ch 24	54	40	−12	Right IFG (BA47)	0.99	$F = 5.21^{*}$	0.71^{**}

$^{*}p < .05$; $^{**}p < .01$; $^{***}p < .001$.

3.4 | Correlation analysis of RT, physiological data, and fNIRS data

The correlations between the RT, physiological, and fNIRS data in the guilty and innocent groups based on the Z-scores of the CIT effect (probe minus irrelevant) were examined. The averaged Z-scores of the HbO changes among the 24 fNIRS channels were used to investigate correlations with the other indicators. The results showed that there were no significant correlations between RT, SCR, HR, and fNIRS data in either the guilty or the innocent group (averaged by channels, see Table 2).

3.5 | Individual analysis using single and combined indicators

Receiver operating characteristic (ROC) curves were constructed using single or combined indicators (RT, SCR, HR, and fNIRS data), providing a measure of

detection efficiency that did not only rely on a single arbitrary cut-off point, but was able to quantify the accuracy of the classification between two stimulus categories using signal detection theory (Ben-Shakhar et al., 1999; Green & Swets, 1966). In the ROC curves, the groups were set as state variables, and the data from the different indicators were set as test variables. The ROC curves provided a series of data showing the "True positive" vs. "False positive" rate at different decision thresholds for specific indicators. Moreover, to investigate whether the use of combined indicators had a higher detection efficiency than the use of single indicators, the area under the curve (AUC), which quantifies the separation between two distributions independently of any specific classification threshold, was computed to represent the detection efficiency of the different indicators. The AUC assumes values between 0 and 1, and an area of 0.5 indicates a lack of differentiation between the two distributions. An area of 1 indicates that there is no overlap between the two distributions, and thus it
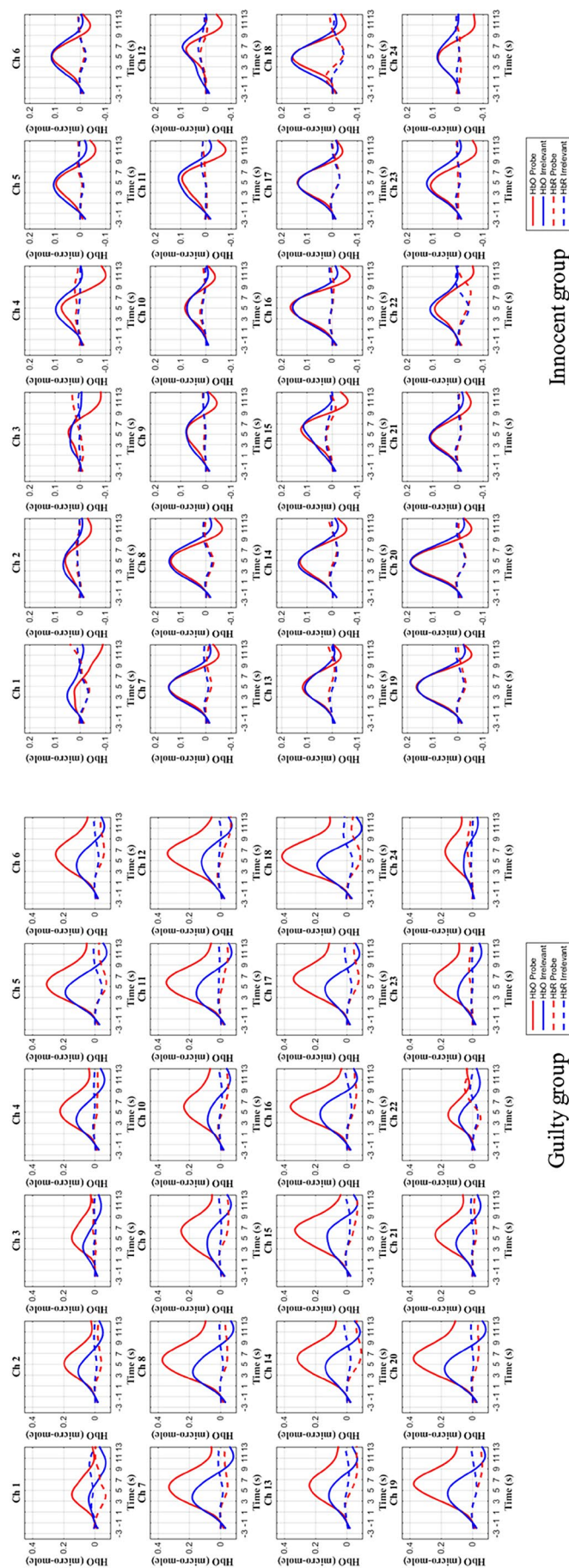
FIGURE 3 The time courses of the grand-averaged hemodynamic (HbO) changes associated with the probe (red solid curve) and irrelevant stimuli (blue solid curve) for the guilty (left) and innocent group (right) participants

FIGURE 4 Mapping of the grand-averaged HbO concentration changes associated with the probe items for the guilty group (top left), the probe items for the innocent group (bottom left), the irrelevant items for the guilty group (top right), and the irrelevant items for the innocent group (bottom right). We found that in the guilty group, the probe items elicited higher hemodynamic responses than the irrelevant stimuli over the prefrontal cortex but not in the innocent group
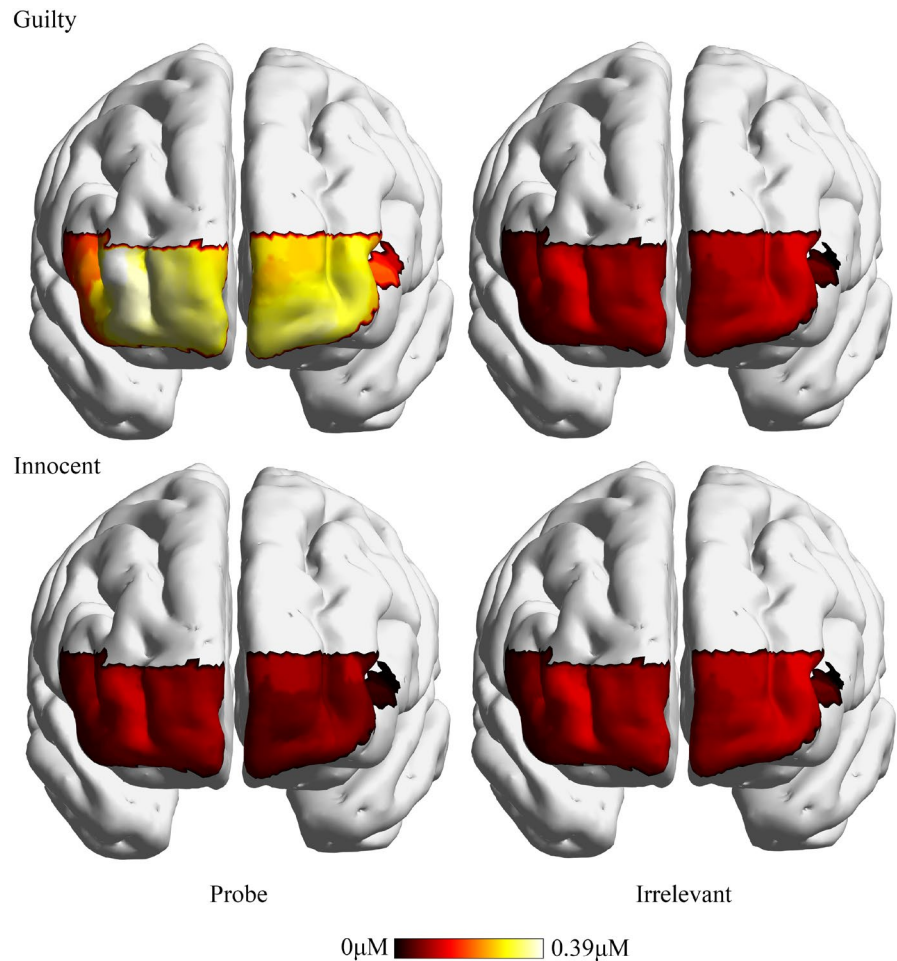

TABLE 2 Correlations between RT, SCR, HR, and fNIRS data

	Guilty group			Innocent group		
	SCR	HR	fNIRS	SCR	HR	fNIRS
RT	0.18	−0.24	0.07	0.24	0.25	0.33
SCR		−0.05	0.14		−0.05	0.10
HR			−0.25			0.12

is possible to detect accurately whether the examinee is guilty or not.

The results of the ROC analyses showed that RT can effectively discriminate guilty from innocent participants above the level of chance (AUC = 0.80, CI = [0.68,0.93], $p < .001$). Physiological indicators, including SCR and HR, could also discriminate guilty from innocent participants above the level of chance (AUC = 0.89, 0.74, CI = [0.81, 0.97], [0.61, 0.86], $ps < .01$). ROC analyses were also conducted on the channels showing significant group × stimulus interaction effects (23 of the 24 channels, $ps < .05$, except channel 3, $p > .05$), with the results showing that all 23 channels' fNIRS data could effectively differentiate between guilty and innocent participants (AUC = [0.69, 0.85], $ps < .05$, Table 1).

In our study, to ensure that the combined indicators could be compared in the same way, they were generated based on the standardized values of CIT effect (probe minus irrelevant), and were averaged in equal weighted value (Hu et al., 2013; Sai et al., 2014). More importantly, the highest AUCs were obtained when all the indicators were combined (AUC = 0.94, CI = [0.89, 1.00], $p < .001$, see Table 3).

4 | DISCUSSION

In the current study, we applied fNIRS to record brain imaging data while quantifying RT, SCR, and HR in a classical three-stimulus CIT. We aimed to test whether combinations of these indicators could improve the deception detection efficiency. Our results showed that probe items elicited significantly longer RTs, larger SCRs, slower HRs, and higher HbO changes in the inferior prefrontal gyrus (IFG), the middle frontal gyrus (MFG), and the superior frontal gyrus (SFG) compared to irrelevant items for participants in the guilty group but not in the innocent group. Our results also showed that single indicators such as RT, SCR, HR, and fNIRS data

Indicators	AUC	95% CI	
		Lower	Upper
fNIRS (24 Channels)	0.82[***]	0.71	0.93
SCR	0.89[***]	0.81	0.97
HR	0.74[**]	0.61	0.86
RT	0.80[***]	0.68	0.93
SCR & fNIRS	0.91[***]	0.84	0.99
HR & fNIRS	0.88[***]	0.80	0.97
RT & fNIRS	0.88[***]	0.78	0.97
SCR, HR & fNIRS	0.94[***]	0.88	1.00
SCR, RT & fNIRS	0.93[***]	0.86	0.99
SCR, HR, RT & fNIRS	0.94[***]	0.89	1.00

*$p < .05$; **$p < .01$; ***$p < .001$.

can effectively detect deception with detection efficiencies of 0.74–0.89. Finally, the combination of RT, SCR, HR, and fNIRS imaging data can elevate the detection efficiency to 0.94.

For fNIRS imaging data, we found that probe items elicited significant higher HbO changes in the IFG, MFG, and SFG compared to irrelevant items in the guilty group participants, but not in the innocent group participants. Our results were consistent with the findings from previous neuroimaging studies (Gamer et al., 2012; Kozel et al., 2005, 2009; Langleben et al., 2005; Suchotzki et al., 2015). It has been suggested that the IFG is involved in inhibitory control during lying (Ding et al., 2012; Suchotzki et al., 2015; Yin & Weber, 2019). In the current study, when presented with their names and hometowns, participants in the guilty group were instructed to deny them by pressing the button, which was contradictory to the truth and required the additional function of inhibitory control. Participants in the innocent group only needed to respond honestly, and thus did not show the activation seen in the guilty group. In addition, it is widely recognized that the MFG plays an important role in response control (Kozel et al., 2005; Mameli et al., 2010; Priori et al., 2008). In the current CIT, participants in the guilty group had to suppress the right response and change it to the wrong response to probe items, while the participants in the innocent group were able to respond with the right answers to all items. Finally, previous studies have demonstrated that the SFG plays an important role in planning of complex actions and goal-processing (Fincham et al., 2002; Li et al., 2013, Ding et al., 2014). In our study, for innocent participants, the goal of this task is simply telling

the truth, while for the guilty participants, they need to lie about probe items: their own names and hometowns. To achieve the goal of lying about probe items, guilty participants need to inhibit the truth and tell the false answer which are more complex than only tell the truth. Therefore, probe items only elicited significantly higher HbO changes in the IFG, MFG, and SFG compared to the irrelevant items in the guilty group, but not in the innocent group.

Our results showed that the physiological measurements can also effectively differentiate guilty and innocent participants. Specifically, we found larger SCR and slower HR values in response to probe items compared to irrelevant items in the guilty participants but not in innocent participants. These findings are in line with previous autonomic-based CIT studies (Meijer et al., 2016; Verschuere et al., 2010). Klein Selle et al. (2016) argued that different physiological measurements in CIT were driven by different mechanisms. Specifically, the SCR reflects orienting response theory, whilst HR and respiration line length (RLL) reflect arousal inhibition (AI) in the fractionation model (Geven et al., 2018; Klein Selle et al., 2016, 2019). In the current study, the guilty participants were presented with probe items that were significant to them, while innocent participants were only presented with unfamiliar stimuli as probe items. Hence, increased SCRs were only apparent in the guilty group and not in the innocent group. In addition, arousal inhibition indicates that executive function allows one to intentionally inhibit a dominant automatic or prepotent response (Miyake et al., 2000). However, this would be at the cost of physiological responses. Accordingly, in our study, participants in the guilty group suppressed their physiological responses to avoid being detected as guilty, resulting in physiological costs and eliciting slower HRs (Pennebaker & Chew, 1985).

RT was also found to effectively distinguish guilty from innocent participants in the current study. This indicated that the guilty participants had significantly longer RTs for probe items compared with irrelevant items but that this did not occur in the innocent group, which is consistent with previous findings on RT-based CIT (Ben-Shakhar, 2012; Seymour et al., 2000). The cognitive view on deception holds that deception consumes more cognitive resources than truth-telling (Vrij, 2008). In the present study, innocent participants only needed to react honestly to all items. In contrast, the participants in the guilty group with crime-related knowledge were required to press the button to indicate that they did not recognize probe items to avoid being identified as guilty, which would consume more cognitive resources. Thus, compared with innocents, there was a longer reaction time to probe items in the guilty participants only.

Our results showed that there were no significant correlations between RT, SCR, HR, and HbO changes in either group, suggesting that the different indicators may operate by different mechanisms (Klein Selle et al., 2016; Matsuda et al., 2011; Suchotzki et al., 2015). RT reflects cognitive effort, SCR reflects orienting response, HR reflects arousal inhibition, and fNIRS reflects response inhibition. In terms of individual detection efficiency, we found that the combination of RT, SCR, HR, and fNIRS data effectively improved the deception efficiency. The AUC for deception detection was 94% when combined with the SCR, HR and fNIRS data. This was higher than the AUC using RT (80%), SCR (88%), HR (75%), or fNIRS (82%) alone. Previous fMRI-based brain imaging studies have also found similar deception detection efficiencies (Hsu et al., 2019; Nuñez et al., 2005). Thus, using combining autonomic measurements with brain imaging, unlike the unimproved AUC in the fMRI-based study (Kozel et al., 2009), our results are comparable to those of fNIRS-based studies that combined autonomic or RT with fNIRS-based brain imaging data to enhance the AUC (Bhutta et al., 2015; Sai et al., 2014). Therefore, in this study, the autonomic and central nervous systems were successfully integrated to detect deception. Indeed, as previous studies suggested (Gamer, 2011), different indicators could associate with different psychophysiological mechanisms and the combination of measures may reduce random error and enhances reliability, thus the combination of multiple measures can elevate the detection efficiency in the current CIT (Gamer et al., 2008; Meijer et al., 2014).

Taken together, the current study demonstrated that single indicators such as RT, SCR, HR, and fNIRS data could be used to effectively detect deception. The combination of SCR, HR, and fNIRS imaging data could increase the AUC to indicate a highly accurate level of deception detection (0.94). These findings show that the combination of multiple indicators is a feasible method to improve deception detection.

ACKNOWLEDGMENTS

CONFLICT OF INTEREST

The authors declare that they have no known competing financial interests or personal relationships that could have appeared to influence the work reported in this paper.

AUTHOR CONTRIBUTIONS

Di Wang: Data curation; formal analysis; visualization; writing – original draft; writing – review and editing. **Chongxiang Wang:** Formal analysis; software; validation; visualization; writing – review and editing. **Xingyu Yi:** Writing – review and editing. **Liyang Sai:** Writing – review and editing. **Genyue Fu:** Resources; supervision; writing – review and editing. **Xiaohong Allison Lin:** Conceptualization; formal analysis; funding acquisition; investigation; methodology; project administration; resources; supervision; writing – review and editing.

ORCID

Di Wang https://orcid.org/0000-0002-7240-5731
Chongxiang Wang https://orcid.org/0000-0002-5109-2254

REFERENCES

Ben-Shakhar, G. (2012). Current research and potential applications of the concealed information test: An overview. *Frontiers in Psychology*, 3, 342. https://doi.org/10.3389/fpsyg.2012.00342

Ben-Shakhar, G., Bar-Hillel, M., & Kremnitzer, M. (2002). Trial by polygraph: Reconsidering the use of the guilty knowledge technique in court. *Law and Human Behavior*, 26(5), 527–541. https://doi.org/10.1023/A:1020204005730

Ben-Shakhar, G., Gronau, N., & Elaad, E. (1999). Leakage of relevant information to innocent examinees in the GKT: An attempt to reduce false-positive outcomes by introducing target stimuli. *Journal of Applied Psychology*, 84(5), 651–660. https://doi.org/10.1037/0021-9010.84.5.651

Bhutta, M. R., Hong, M. J., Kim, Y.-H., & Hong, K.-S. (2015). Single-trial lie detection using a combined fNIRS-polygraph system. *Frontiers in Psychology*, 6, 709. https://doi.org/10.3389/fpsyg.2015.00709

Bles, M., & Haynes, J.-D. (2008). Detecting concealed information using brain-imaging technology. *Neurocase*, 14(1), 82–92. https://doi.org/10.1080/13554790801992784

Cope, M., & Delpy, D. T. (1988). System for long-term measurement of cerebral blood and tissue oxygenation on newborn infants by near infra-red transillumination. *Medical and Biological Engineering and Computing*, 26(3), 289–294. https://doi.org/10.1007/BF02447083

De Clercq, A., Verschuere, B., De Vlieger, P., & Crombez, G. (2006). Psychophysiological analysis (PSPHA): A modular script-based program for analyzing psychophysiological data. *Behavior Research Methods*, 38(3), 504–510. https://doi.org/10.3758/BF03192805

DePaulo, B. M., Kashy, D. A., Kirkendol, S. E., Wyer, M. M., & Epstein, J. A. (1996). Lying in everyday life. *Journal of Personality and Social Psychology*, 70(5), 979–995. https://doi.org/10.1037/0022-3514.70.5.979

Ding, X. P., Du, X., Lei, D., Hu, C. S., Fu, G., & Chen, G. (2012). The neural correlates of identity faking and concealment: An fMRI study. *PLoS One*, 7(11), e48639. https://doi.org/10.1371/journal.pone.0048639

Ding, X. P., Gao, X., Fu, G., & Lee, K. (2013). Neural correlates of spontaneous deception: A functional near-infrared spectroscopy (fNIRS)study. *Neuropsychologia*, 51(4), 704–712. https://doi.org/10.1016/j.neuropsychologia.2012.12.018

Ding, X. P., Sai, L., Fu, G., Liu, J., & Lee, K. (2014). Neural correlates of second-order verbal deception: A functional near-infrared spectroscopy (fNIRS) study. *NeuroImage*, *87*, 505–514. https://doi.org/10.1016/j.neuroimage.2013.10.023

Farah, M. J., Hutchinson, J. B., Phelps, E. A., & Wagner, A. D. (2014). Functional MRI-based lie detection: Scientific and societal challenges. *Nature Reviews Neuroscience*, *15*(2), 123–131. https://doi.org/10.1038/nrn3665

Farwell, L. A., & Donchin, E. (1991). The truth will out: Interrogative polygraphy ("lie detection") with event-related brain potentials. *Psychophysiology*, *28*(5), 531–547. https://doi.org/10.1111/j.1469-8986.1991.tb01990.x

Fincham, J. M., Carter, C. S., van Veen, V., Stenger, V. A., & Anderson, J. R. (2002). Neural mechanisms of planning: A computational analysis using event-related fMRI. *Proceedings of the National Academy of Sciences*, *99*(5), 3346–3351. https://doi.org/10.1073/pnas.052703399

Gamer, M. (2011). Detecting of deception and concealed information using neuroimaging techniques. In *Memory detection: Theory and application of the concealed information test* (pp. 90–113). Cambridge University Press.

Gamer, M., Bauermann, T., Stoeter, P., & Vossel, G. (2007). Covariations among fMRI, skin conductance, and behavioral data during processing of concealed information. *Human Brain Mapping*, *28*(12), 1287–1301. https://doi.org/10.1002/hbm.20343

Gamer, M., & Berti, S. (2010). Task relevance and recognition of concealed information have different influences on electrodermal activity and event-related brain potentials. *Psychophysiology*, *47*(2), 355–364. https://doi.org/10.1111/j.1469-8986.2009.00933.x

Gamer, M., Klimecki, O., Bauermann, T., Stoeter, P., & Vossel, G. (2012). FMRI-activation patterns in the detection of concealed information rely on memory-related effects. *Social Cognitive and Affective Neuroscience*, *7*(5), 506–515. https://doi.org/10.1093/scan/nsp005

Gamer, M., Verschuere, B., Crombez, G., & Vossel, G. (2008). Combining physiological measures in the detection of concealed information. *Physiology & Behavior*, *95*(3), 333–340. https://doi.org/10.1016/j.physbeh.2008.06.011

Ganis, G., Rosenfeld, J. P., Meixner, J., Kievit, R. A., & Schendan, H. E. (2011). Lying in the scanner: Covert countermeasures disrupt deception detection by functional magnetic resonance imaging. *NeuroImage*, *55*(1), 312–319. https://doi.org/10.1016/j.neuroimage.2010.11.025

Geven, L. M., Klein Selle, N., Ben-Shakhar, G., Kindt, M., & Verschuere, B. (2018). Self-initiated versus instructed cheating in the physiological concealed information test. *Biological Psychology*, *138*, 146–155. https://doi.org/10.1016/j.biopsycho.2018.09.005

Green, D. M., & Swets, J. A. (1966). *Signal detection theory and psychophysics*. Wiley http://gen.lib.rus.ec/book/index.php?md5=bbbbc96c5518f7355fea0ba577f6276b

Gronau, N., Ben-Shakhar, G., & Cohen, A. (2005). Behavioral and physiological measures in the detection of concealed information. *Journal of Applied Psychology*, *90*(1), 147–158. https://doi.org/10.1037/0021-9010.90.1.147

Homae, F., Watanabe, H., Nakano, T., & Taga, G. (2007). Prosodic processing in the developing brain. *Neuroscience Research*, *59*(1), 29–39. https://doi.org/10.1016/j.neures.2007.05.005

Hsu, C.-W., Begliomini, C., Dall'Acqua, T., & Ganis, G. (2019). The effect of mental countermeasures on neuroimaging-based concealed information tests. *Human Brain Mapping*, *40*(10), 2899–2916. https://doi.org/10.1002/hbm.24567

Hu, X., Evans, A., Wu, H., Lee, K., & Fu, G. (2013). An interfering dot-probe task facilitates the detection of mock crime memory in a reaction time (RT)-based concealed information test. *Acta Psychologica*, *142*(2), 278–285.

Huppert, T. J., Diamond, S. G., Franceschini, M. A., & Boas, D. A. (2009). HomER: A review of time-series analysis methods for near-infrared spectroscopy of the brain. *Applied Optics*, *48*(10), D280–D298. https://doi.org/10.1364/AO.48.00D280

Iacono, W. G., & Lykken, D. T. (1997). The validity of the lie detector: Two surveys of scientific opinion. *Journal of Applied Psychology*, *82*(3), 426–433. https://doi.org/10.1037/0021-9010.82.3.426

Klein Selle, N., Agari, N., & Ben-Shakhar, G. (2019). Hide or seek? Physiological responses reflect both the decision and the attempt to conceal information. *Psychological Science*, *30*(10), 1424–1433. https://doi.org/10.1177/0956797619864598

Klein Selle, N., Verschuere, B., Kindt, M., Meijer, E., & Ben-Shakhar, G. (2016). Orienting versus inhibition in the concealed information test: Different cognitive processes drive different physiological measures. *Psychophysiology*, *53*(4), 579–590. https://doi.org/10.1111/psyp.12583

Kozel, F. A., Johnson, K. A., Grenesko, E. L., Laken, S. J., Kose, S., Lu, X., Pollina, D., Ryan, A., & George, M. S. (2009). Functional MRI detection of deception after committing a mock sabotage crime. *Journal of Forensic Sciences*, *54*(1), 220–231. https://doi.org/10.1111/j.1556-4029.2008.00927.x

Kozel, F. A., Johnson, K. A., Mu, Q., Grenesko, E. L., Laken, S. J., & George, M. S. (2005). Detecting deception using functional magnetic resonance imaging. *Biological Psychiatry*, *58*(8), 605–613. https://doi.org/10.1016/j.biopsych.2005.07.040

Li, W., Qin, W., Liu, H., Fan, L., Wang, J., Jiang, T., & Yu, C. (2013). Subregions of the human superior frontal gyrus and their connections. *NeuroImage*, *78*, 46–58. https://doi.org/10.1016/j.neuroimage.2013.04.011

Langleben, D. D., Loughead, J. W., Bilker, W. B., Ruparel, K., Childress, A. R., Busch, S. I., & Gur, R. C. (2005). Telling truth from lie in individual subjects with fast event-related fMRI. *Human Brain Mapping*, *26*(4), 262–272. https://doi.org/10.1002/hbm.20191

Lin, X. A., Wang, C., Zhou, J., Sai, L., & Fu, G. (2021). Neural correlates of spontaneous deception in a non-competitive interpersonal scenario: A functional near-infrared spectroscopy (fNIRS) study. *Brain and Cognition*, *150*, 105704. https://doi.org/10.1016/j.bandc.2021.105704

Lin, X., Sai, L., & Yuan, Z. (2018). Detecting concealed information with fused electroencephalography and functional near-infrared spectroscopy. *Neuroscience*, *386*, 284–294. https://doi.org/10.1016/j.neuroscience.2018.06.049

Lin, X., Xu, S., Ieong, H. F.-H., & Yuan, Z. (2017). Optical mapping of prefrontal activity in pathological gamblers. *Applied Optics*, *56*(21), 5948–5953. https://doi.org/10.1364/ao.56.005948

Liu, T., Saito, G., Lin, C., & Saito, H. (2017). Inter-brain network underlying turn-based cooperation and competition: A hyperscanning study using near-infrared spectroscopy. *Scientific Reports*, *7*(1), 8684. https://doi.org/10.1038/s41598-017-09226-w

Lykken, D. T. (1960). The validity of the guilty knowledge technique: The effects of faking. *Journal of Applied Psychology*, *44*(4), 258–262. https://doi.org/10.1037/h0044413

Mameli, F., Mrakic-Sposta, S., Vergari, M., Fumagalli, M., Macis, M., Ferrucci, R., Nordio, F., Consonni, D., Sartori, G., & Priori, A. (2010). Dorsolateral prefrontal cortex specifically processes general – But not personal – Knowledge deception: Multiple brain networks for lying. *Behavioural Brain Research*, *211*(2), 164–168. https://doi.org/10.1016/j.bbr.2010.03.024

Matsuda, I., Hirota, A., Ogawa, T., Takasawa, N., & Shigemasu, K. (2009). Within-individual discrimination on the concealed information test using dynamic mixture modeling. *Psychophysiology*, *46*(2), 439–449. https://doi.org/10.1111/j.1469-8986.2008.00781.x

Matsuda, I., Nittono, H., & Allen, J. (2012). The current and future status of the concealed information test for field use. *Frontiers in Psychology*, *3*, 532. https://doi.org/10.3389/fpsyg.2012.00532

Matsuda, I., Nittono, H., & Ogawa, T. (2011). Event-related potentials increase the discrimination performance of the autonomic-based concealed information test. *Psychophysiology*, *48*(12), 1701–1710. https://doi.org/10.1111/j.1469-8986.2011.01266.x

Meijer, E. H., Klein Selle, N., Elber, L., & Ben-Shakhar, G. (2014). Memory detection with the concealed information test: A meta analysis of skin conductance, respiration, heart rate, and P300 data. *Psychophysiology*, *51*(9), 879–904. https://doi.org/10.1111/psyp.12239

Meijer, E. H., Smulders, F. T., Johnston, J. E., & Merckelbach, H. L. (2007). Combining skin conductance and forced choice in the detection of concealed information. *Psychophysiology*, *44*(5), 814–822. https://doi.org/10.1111/j.1469-8986.2007.00543.x

Meijer, E. H., Verschuere, B., Gamer, M., Merckelbach, H., & Ben-Shakhar, G. (2016). Deception detection with behavioral, autonomic, and neural measures: Conceptual and methodological considerations that warrant modesty. *Psychophysiology*, *53*(5), 593–604. https://doi.org/10.1111/PSYP.12609

Miyake, A., Friedman, N. P., Emerson, M. J., Witzki, A. H., Howerter, A., & Wager, T. D. (2000). The unity and diversity of executive functions and their contributions to complex "frontal lobe" tasks: A latent variable analysis. *Cognitive Psychology*, *41*(1), 49–100. https://doi.org/10.1006/cogp.1999.0734

Nahari, G., & Ben-Shakhar, G. (2011). Psychophysiological and behavioral measures for detecting concealed information: The role of memory for crime details. *Psychophysiology*, *48*(6), 733–744. https://doi.org/10.1111/j.1469-8986.2010.01148.x

Nuñez, J. M., Casey, B. J., Egner, T., Hare, T., & Hirsch, J. (2005). Intentional false responding shares neural substrates with response conflict and cognitive control. *NeuroImage*, *25*(1), 267–277. 15. https://doi.org/10.1016/j.neuroimage.2004.10.041

Pennebaker, J. W., & Chew, C. H. (1985). Behavioral inhibition and electrodermal activity during deception. *Journal of Personality and Social Psychology*, *49*(5), 1427–1433. https://doi.org/10.1037/0022-3514.49.5.1427

Priori, A., Mameli, F., Cogiamanian, F., Marceglia, S., Tiriticco, M., Mrakic-Sposta, S., Ferrucci, R., Zago, S., Polezzi, D., & Sartori, G. (2008). Lie-specific involvement of dorsolateral prefrontal cortex in deception. *Cerebral Cortex*, *18*(2), 451–455. https://doi.org/10.1093/cercor/bhm088

Rosenfeld, J. P., Biroschak, J. R., & Furedy, J. J. (2006). P300-based detection of concealed autobiographical versus incidentally acquired information in target and non-target paradigms. *International Journal of Psychophysiology*, *60*(3), 251–259. https://doi.org/10.1016/j.ijpsycho.2005.06.002

Rosenfeld, J. P., Soskins, M., Bosh, G., & Ryan, A. (2004). Simple, effective countermeasures to P300-based tests of detection of concealed information. *Psychophysiology*, *41*(2), 205–219. https://doi.org/10.1111/j.1469-8986.2004.00158.x

Sai, L., Bellucci, G., Wang, C., Fu, G., Camilleri, J. A., Eickhoff, S. B., & Krueger, F. (2021). Neural mechanisms of deliberate dishonesty: Dissociating deliberation from other control processes during dishonest behaviors. *Proceedings of the National Academy of Sciences*, *118*(43), e2109208118. https://doi.org/10.1073/pnas.2109208118

Sai, L., Zhou, X., Ding, X. P., Fu, G., & Sang, B. (2014). Detecting concealed information using functional near-infrared spectroscopy. *Brain Topography*, *27*(5), 652–662. https://doi.org/10.1007/s10548-014-0352-z

Seymour, T. L., Seifert, C. M., Shafto, M. G., & Mosmann, A. L. (2000). Using response time measures to assess "guilty knowledge". *Journal of Applied Psychology*, *85*(1), 30–37. https://doi.org/10.1037/0021-9010.85.1.30

Singh, A. K., & Dan, I. (2006). Exploring the false discovery rate in multichannel NIRS. *NeuroImage*, *33*(2), 542–549. https://doi.org/10.1016/j.neuroimage.2006.06.047

Singh, A. K., Okamoto, M., Dan, H., Jurcak, V., & Dan, I. (2005). Spatial registration of multichannel multi-subject fNIRS data to MNI space without MRI. *NeuroImage*, *27*(4), 842–851. https://doi.org/10.1016/j.neuroimage.2005.05.019

Suchotzki, K., Verschuere, B., Peth, J., Crombez, G., & Gamer, M. (2015). Manipulating item proportion and deception reveals crucial dissociation between behavioral, autonomic, and neural indices of concealed information. *Human Brain Mapping*, *36*(2), 427–439. https://doi.org/10.1002/hbm.22637

Suchotzki, K., Verschuere, B., Van Bockstaele, B., Ben-Shakhar, G., & Crombez, G. (2017). Lying takes time: A meta-analysis on reaction time measures of deception. *Psychological Bulletin*, *143*(4), 428–453. https://doi.org/10.1037/bul0000087

Synnott, J., Dietzel, D., & Ioannou, M. (2015). A review of the polygraph: History, methodology and current status. *Crime Psychology Review*, *1*(1), 59–83. https://doi.org/10.1080/23744006.2015.1060080

Tian, F., Sharma, V., Kozel, F. A., & Liu, H. (2009). Functional near-infrared spectroscopy to investigate hemodynamic responses to deception in the prefrontal cortex. *Brain Research*, *1303*, 120–130. https://doi.org/10.1016/j.brainres.2009.09.085

Verschuere, B., Crombez, G., Degroote, T., & Rosseel, Y. (2010). Detecting concealed information with reaction times: Validity and comparison with the polygraph. *Applied Cognitive Psychology*, *24*(7), 991–1002. https://doi.org/10.1002/acp.1601

Verschuere, B., Crombez, G., Koster, E. H. W., Van Bockstaele, B., & De Clercq, A. (2007). Startling secrets: Startle eye blink modulation by concealed crime information. *Biological Psychology*, *76*(1), 52–60. https://doi.org/10.1016/j.biopsycho.2007.06.001

Vrij, A. (2008). *Detecting lies and deceit: Pitfalls and opportunities*. John Wiley & Sons.

Xia, M., Wang, J., & He, Y. (2013). BrainNet viewer: A network visualization tool for human brain connectomics. *PLoS One*, *8*(7), e68910. https://doi.org/10.1371/journal.pone.0068910

Yin, L., & Weber, B. (2019). I lie, why don't you: Neural mechanisms of individual differences in self-serving lying. *Human Brain Mapping*, *40*(4), 1101–1113. https://doi.org/10.1002/hbm.24432

Yu, J., Tao, Q., Zhang, R., Chan, C. C. H., & Lee, T. M. C. (2019). Can fMRI discriminate between deception and false memory? A meta-analytic comparison between deception and false memory studies. *Neuroscience & Biobehavioral Reviews*, *104*(6), 43–55. https://doi.org/10.1016/j.neubiorev.2019.06.027

Zhang, M., Liu, T., Pelowski, M., & Yu, D. (2017). Gender difference in spontaneous deception: A hyperscanning study using functional near-infrared spectroscopy. *Scientific Reports*, *7*(1), 7508. https://doi.org/10.1038/s41598-017-06764-1

SUPPORTING INFORMATION

Additional supporting information may be found in the online version of the article at the publisher's website.

TABLE S1 Statistical analysis using fNIRS oxyhemoglobin (HbO) changes (including main effects, interaction effect, and simple effect)